death or last clinical evaluation. The mean follow-up interval was 50 months (range 1–196 months).

Immunohistochemistry

The method of immunohistochemistry and scoring of immunoreactivity for Rsf-1 expression were previously described (13,14). Briefly, 4 μm sections were cut from the tissue microarray blocks. Antigen retrieval was performed on deparaffinized sections by steaming them in citrate buffer (pH 6.0). A monoclonal anti-Rsf-1 antibody, clone 5H2/E4 (Upstate, Lake Placid, NY), was used at an optimal dilution of 1:2000 as previously determined (13,14) and a monoclonal anti-NAC1 antibody was used at a dilution of 1:250 (16). The sections were incubated with the antibodies for 2 hours at room temperature, followed by the EnVision+ System (DAKO, Carpinteria, California) using the peroxidase method. An isotype-matched control antibody (MN-4) was used in parallel (17). Our previous studies had shown that the distribution of Rsf-1 immunoreactivity was always homogeneous within a tumor; therefore, we used an intensity score ranging from 0 to 4+ to evaluate Rsf-1 immunoreactivity in tumors as previously described (14). A positive reaction for both Rsf-1 and NAC1 was defined as discrete localization of the chromogen in the nuclei. The tissues were scored in a blinded fashion without the knowledge of clinical information.

Rsf-1 gene knockdown using small hairpin RNA

Ovarian clear cell adenocarcinoma cell lines, ES2 and JHOC5, were used in this study. ES2 was obtained from the American Type Culture Collection (Rockville,, MD, USA); JHOC5 was a kind gift from Dr. Kentaro Nakayama, Shimane University, Japan. Both cell lines used in this study were cultured in RPMI 1640 containing 5% fetal bovine serum.

In order to confirm the specificity of the anti-Rsf-1 antibody used for immunohistochemistry, we performed Rsf-1 knockdown by transduction of two small hairpin RNAs (shRNA) and evaluated the knockdown efficiency by Western blot. The antibody specificity was indicated by reduced protein expression corresponding to Rsf-1 after gene knockdown based on western blot analysis using the same anti-Rsf-1 antibody as used in immunohistochemistry. We used lentivirus carrying the Rsf-1 shRNA sequence templates (CCGGCCAGTTCTGAAC TTTGAAGATCTCGAGATCTTCAAAGTTCAGAACT) and (CCGGCTTCTGAGA CAAAGGGTTCTACTCGAGTAGAACCCTTTGTCTCAGA), and a control shRNA sequence template, which were inserted into the lentiviral plasmid (pLKO.1-puro). Cells were washed and harvested 24 hours after transfection for protein and mRNA extraction.

For Western blot analysis, protein lysates were separated by 4% to 20% Tris-glycine gel electrophoresis and transferred onto polyvinylidene difluoride membranes using a semidry apparatus (Bio-Rad). After blocking, membranes were incubated with the anti-Rsf-1 (clone 5H2/E4) primary antibody at 4°C overnight followed by incubation with horseradish peroxidase (HRP)-conjugated secondary antibody. Protein bands were detected with Amersham ECL Western blotting detection reagents (GE Healthcare). Antibody reacting to anti-GAPDH was used to evaluate the amount of GAPDH as a loading control. Western blot analysis showed a reduced protein band corresponding to Rsf-1 in cells transfected with Rsf-1 shRNA as compared to control shRNA transfected cells, indicating the specificity of the anti-Rsf-1 antibody (Fig. 1).

Statistical Analysis

Statistical analysis was performed using the χ^2-test. Overall survival of CCC cases was calculated using the Kaplan-Meier method, and statistical analyses were performed using the

log-rank test. Statistical analyses were performed with StatView 5.0 software (SAS Institute, Cary, NC) and $P < 0.05$ was considered statistically significant.

Results

Expression of Rsf-1 in ovarian clear cell carcinomas

Results of Rsf-1 immunohistochemistry in CCCs are summarized in Table 1. Rsf-1 immunoreactivity was detected exclusively in nuclei of almost all tumor cells. Positive immunoreactivity of Rsf-1 was observed in 73 (82%) of 89 cases. Specifically, 16 (18%), 53 (60%), and 19 (21%) of 89 cases had a staining score of 0, 1+, and 2+, respectively. Only one case exhibited intense nuclear staining (3+). Histological features in representative cases with different Rsf-1 immunostaining intensities including 0, 1+, and 2+ are shown in Fig. 2. There was no correlation between Rsf-1 expression and histological pattern and nuclear atypia of the CCC cases.

Correlation of Rsf-1 expression with clinical features

Since Rsf-1 expression has been reported to play a tumor-promoting role in ovarian cancer, we analyzed the possible correlation of Rsf-1 expression with clinical characteristics in CCC (Table 2). Statistically significant correlations were observed between Rsf-1 immunostaining intensity (score > 1) and lymph node involvement ($P = 0.023$). Furthermore, Rsf-1 immunostaining intensity (score > 1) was associated with advanced stage disease (Stage III/IV) ($P = 0.0088$). In fact, none of the Rsf-1 negative cases presented at an advanced stage. The frequency of peritoneal dissemination was higher in Rsf-1 positive cases (12/65), compared to Rsf-1 negative cases (1/14) but the difference was not statistically significant ($P = 0.3$). As a control we also assessed the expression of Nac1, a nuclear protein involved in transcription regulation, in the same set of CCC. We found that there was no significant association of Nac1 expression and any clinical feature including presentation stage or lymph node metastasis status ($p > 0.1$) (data not shown). Kaplan-Meier analyses were performed to determine if there was a correlation between Rsf-1 expression and clinical outcome. We first assessed the association between tumor stage and overall survival in CCCs, and demonstrated that stage III/IV cases ($n = 20$) had a poorer prognosis than stage I/II cases ($n = 47$) ($P < 0.0001$) (Fig. 3). However, Kaplan-Meier analysis did not reveal a significant difference in survival between Rsf-1 positive and negative cases ($P = 0.42$).

Discussion

An increase in DNA copy number at the chromosome 11q13.5 locus containing *Rsf-1* (*HBXAP*) is detected in several types of human cancer including ovarian high-grade serous carcinoma. *Rsf-1* (*HBXAP*) encodes for a cellular nuclear protein that binds to hSNF2H (18), forming a chromatin remodeling protein complex called RSF (Remodeling and Spacing Factor) (19,20). Rsf-1 (HBXAP) has been shown to function as a histone chaperone in the nuclei while its binding partner, hSNF2H, possesses nucleosome-dependent ATPase activity (21). The Rsf-1/hSNF2H complex (RSF complex) mediates ATP-dependent chromatin remodeling, which alters the chromatin structure or positioning of nucleosomes (20). At the cellular level, RSF participates in chromatin remodeling in response to a variety of growth signals and environmental cues. Such nucleosome remodeling is required for transcriptional activation or repression (22,23,24), DNA replication (25), and cell cycle progression (26).

In this study, we used a well characterized anti-Rsf-1 antibody to study the expression pattern of Rsf-1 in CCC, and provided new evidence that expression of Rsf-1 was associated with advanced clinical stages and with the status of lymph node metastasis in CCC. The

findings suggest a biological role for Rsf-1 in disease aggressiveness in this type of ovarian carcinoma. Interestingly, we have previously reported that chromosome 11q13.5 amplification and overexpression in cases of ovarian high-grade serous carcinoma contributes to shorter overall survival compared to cases without amplification. A possible mechanism was thought to be related to the de novo paclitaxel resistance rendered by Rsf-1 overexpression (27). Although Kaplan-Meier survival analysis did not show statistically significant difference between Rsf-1 positive CCC cases and Rsf-1 negative CCC cases, long-term prognosis of Rsf-1 positive cases appears to be slightly worse than Rsf-1 negative cases. However, the number of Rsf-1 negative CCC cases in our series was relatively small, and we believe that analysis in larger series on CCCs is required to conclude if Rsf-1 overexpression predicts worse overall survival in CCCs. Furthermore, our study suggests a potential use of Rsf-1 immunoreactivity as a biomarker that may prove useful for predicting clinical outcomes in primary CCC, including higher clinical stages, and for predicting the risk of developing lymph node metastasis. To this end, several proteins including IGF2BP3 (IMP3) (11) and annexin A4 (12) have been reported as new markers associated with treatment outcomes in CCC. Thus, a panel of different markers including Rsf-1 could be tested in future clinical trials to determine their potential to be used in the management of CCC patients.

In the current report, we observed that, with a single exception, the immunostaining intensity score of Rsf-1 was less than 3+ in all cases analyzed. This finding provides an independent confirmation of our previous observation in another, smaller set of CCC samples in which we demonstrated that the majority of CCCs showed an immunostaining intensity score of 1+ or 2+ (14). In fact, the percentage of Rsf-1 positive and negative cases is very similar between the current and previous reports. Moreover, analysis of SNP arrays performed on affinity-purified CCC specimens did not show an increase in DNA copy number at chromosome 11q13.5, indicating that *Rsf-1* is rarely amplified in CCC (28). The above findings in CCC are in sharp contrast to those in high-grade serous carcinoma (14), and underscore the distinct molecular pathways in developing CCC and high-grade serous carcinoma (reviewed in (29)). It is also noteworthy that endometrioid and mucinous carcinomas of the ovary express Rsf-1 much less frequently as compared to CCCs and high-grade serous carcinoma. Only 49% of endometrioid carcinomas and 48% of mucinous carcinomas were Rsf-1 positive, and the intensity scores of positive cases were mostly 1+ and 2+.

In conclusion, using immunohistochemistry with an Rsf-1 specific antibody we demonstrated that the presence of Rsf-1 immunoreactivity is significantly associated with advanced stage and lymph node metastasis in primary CCCs. Our findings suggest Rsf-1 expression may contribute to disease aggressiveness in CCC, and warrant further study of the biological role of Rsf-1 in progression of CCC.

Acknowledgments

This study was supported by NIH/NCI grant CA129080 and the International Training Program from the Japan Society for the Promotion of Science.

References

1. Chan JK, Teoh D, Hu JM, Shin JY, Osann K, Kapp DS. Do clear cell ovarian carcinomas have poorer prognosis compared to other epithelial cell types? A study of 1411 clear cell ovarian cancers. Gynecol Oncol 2008;109:370–376. [PubMed: 18395777]
2. Ushijima K. Current status of gynecologic cancer in Japan. J Gynecol Oncol 2009;20:67–71. [PubMed: 19590716]

3. Takano M, Kikuchi Y, Yaegashi N, et al. Clear cell carcinoma of the ovary: a retrospective multicentre experience of 254 patients with complete surgical staging. Br J Cancer 2006;94:1369–1374. [PubMed: 16641903]
4. Mizuno M, Kikkawa F, Shibata K, et al. Long-term follow-up and prognostic factor analysis in clear cell adenocarcinoma of the ovary. J Surg Oncol 2006;94:138–143. [PubMed: 16847906]
5. Jenison EL, Montag AG, Griffiths CT, et al. Clear cell adenocarcinoma of the ovary: a clinical analysis and comparison with serous carcinoma. Gynecol Oncol 1989;32:65–71. [PubMed: 2642454]
6. Veras E, Mao TL, Ayhan A, et al. Cystic and adenofibromatous clear cell carcinomas of the ovary: distinctive tumors that differ in their pathogenesis and behavior: a clinicopathologic analysis of 122 cases. Am J Surg Pathol 2009;33:844–853. [PubMed: 19342944]
7. Fukunaga M, Nomura K, Ishikawa E, Ushigome S. Ovarian atypical endometriosis: its close association with malignant epithelial tumours. Histopathology 1997;30:249–255. [PubMed: 9088954]
8. Erzen M, Rakar S, Klancnik B, Syrjanen K. Endometriosis-associated ovarian carcinoma (EAOC): an entity distinct from other ovarian carcinomas as suggested by a nested case-control study. Gynecol Oncol 2001;83:100–108. [PubMed: 11585420]
9. Sato N, Tsunoda H, Nishida M, et al. Loss of heterozygosity on 10q23.3 and mutation of the tumor suppressor gene PTEN in benign endometrial cyst of the ovary: possible sequence progression from benign endometrial cyst to endometrioid carcinoma and clear cell carcinoma of the ovary. Cancer Res 2000;60:7052–7056. [PubMed: 11156411]
10. Marquez RT, Baggerly KA, Patterson AP, et al. Patterns of gene expression in different histotypes of epithelial ovarian cancer correlate with those in normal fallopian tube, endometrium, and colon. Clin Cancer Res 2005;11:6116–6126. [PubMed: 16144910]
11. Kobel M, Xu H, Bourne PA, et al. IGF2BP3 (IMP3) expression is a marker of unfavorable prognosis in ovarian carcinoma of clear cell subtype. Mod Pathol 2009;22:469–475. [PubMed: 19136932]
12. Aoki D, Oda Y, Hattori S, et al. Overexpression of class III beta-tubulin predicts good response to taxane-based chemotherapy in ovarian clear cell adenocarcinoma. Clin Cancer Res 2009;15:1473–1480. [PubMed: 19228748]
13. Shih IM, Sheu JJ, Santillan A, et al. Amplification of a chromatin remodeling gene, Rsf-1/HBXAP, in ovarian carcinoma. Proc Natl Acad Sci U S A 2005;102:14004–14009. [PubMed: 16172393]
14. Mao TL, Hsu CY, Yen MJ, et al. Expression of Rsf-1, a chromatin-remodeling gene, in ovarian and breast carcinoma. Hum Pathol 2006;37:1169–1175. [PubMed: 16938522]
15. Shih IM, Davidson B. Pathogenesis of ovarian cancer: clues from selected overexpressed genes. Future Oncol 2009;5:1641–1657. [PubMed: 20001801]
16. Nakayama K, Nakayama N, Davidson B, et al. A BTB/POZ protein, NAC-1, is related to tumor recurrence and is essential for tumor growth and survival. Proc Natl Acad Sci U S A 2006 Dec 5;103:18739–18744. [PubMed: 17130457]
17. Shih IM, Nesbit M, Herlyn M, et al. A new Mel-CAM (CD146)-specific monoclonal antibody, MN-4, on paraffin-embedded tissue. Mod Pathol 1998;11:1098–1106. [PubMed: 9831208]
18. Sheu JJ, Choi JH, Yildiz I, et al. The Roles of Human Sucrose Nonfermenting Protein 2 Homologue in the Tumor-Promoting Functions of Rsf-1. Cancer Res 2008;68:4050–4057. [PubMed: 18519663]
19. LeRoy G, Loyola A, Lane WS, Reinberg D. Purification and characterization of a human factor that assembles and remodels chromatin. J Biol Chem 2000;275:14787–14790. [PubMed: 10747848]
20. Loyola A, Huang J-Y, LeRoy G, et al. Functional Analysis of the Subunits of the Chromatin Assembly Factor RSF. Mol Cell Biol 2003;23:6759–6768. [PubMed: 12972596]
21. Aihara T, Miyoshi Y, Koyama K, et al. Cloning and mapping of SMARCA5 encoding hSNF2H, a novel human homologue of Drosophila ISWI. Cytogenet Cell Genet 1998;81:191–193. [PubMed: 9730600]
22. Shamay M, Barak O, Shaul Y. HBXAP, a novel PHD-finger protein, possesses transcription repression activity. Genomics 2002;79:523–529. [PubMed: 11944984]

23. Shamay M, Barak O, Doitsh G, Ben-Dor I, Shaul Y. Hepatitis B virus pX interacts with HBXAP, a PHD finger protein to coactivate transcription. J Biol Chem 2002;277:9982–9988. [PubMed: 11788598]

24. Vignali M, Hassan AH, Neely KE, Workman JL. ATP-dependent chromatin-remodeling complexes. Mol Cell Biol 2000;20:1899–1910. [PubMed: 10688638]

25. Flanagan JF, Peterson CL. A role for the yeast SWI/SNF complex in DNA replication. Nucleic Acids Res 1999;27:2022–2028. [PubMed: 10198436]

26. Cosma MP, Tanaka T, Nasmyth K. Ordered recruitment of transcription and chromatin remodeling factors to a cell cycle- and developmentally regulated promoter. Cell 1999;97:299–311. [PubMed: 10319811]

27. Choi JH, Sheu JJ, Guan B, et al. Functional analysis of 11q13.5 amplicon identifies Rsf-1 (HBXAP) as a gene involved in paclitaxel resistance in ovarian cancer. Cancer Res 2009;69:1407–1415. [PubMed: 19190325]

28. Kuo K, Mao T, Feng Y, et al. DNA copy number profiles in affinity-purified ovarian clear cell carcinoma. Clin Cancer Res. 2010 April 1; 2010 issue.

29. Cho KR, Shih IM. Ovarian cancer. Annu Rev Pathol Mech Dis 2009;4:287–313.

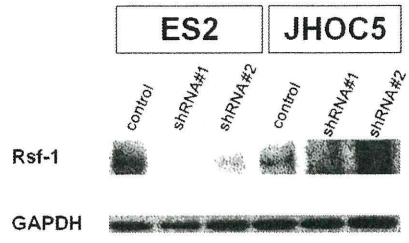

Fig. 1.

Rsf-1 expression in ovarian clear cell carcinoma cell lines, ES2 and JHOC5

Western blot analysis showed a reduced protein band corresponding to Rsf-1 protein in Rsf-1 specific shRNA transfected cells as compared to control shRNA transfected cells, indicating the specificity of the anti-Rsf-1 antibody.

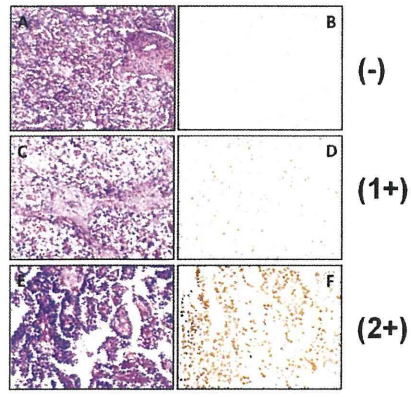

Fig. 2.

Rsf-1 immunoreactivity in representative ovarian clear cell carcinomas

(A, B) Microscopic view of an ovarian clear cell carcinoma showing negative immunoreactivity for Rsf-1. (C, D) A case of ovarian clear cell carcinoma with 1+ immunostaining intensity for Rsf-1. (E, F) A clear cell carcinoma with 2+ immunoreactivity for Rsf-1. A, C and E: hematoxylin and eosin stained sections; B, D and F: Rsf-1 stained sections.

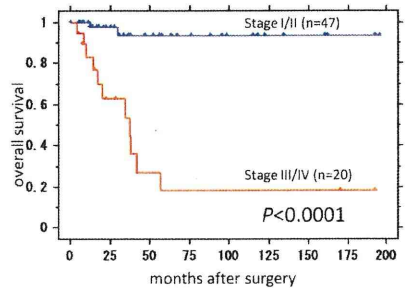

Fig. 3.

Kaplan-Meier survival curve analysis shows that patients with stage III/IV ovarian clear cell carcinoma have a significantly worse overall survival rate than those with stage I/II ovarian clear cell carcinoma ($P< 0.0001$).

Table 1

Rsf-1 expression in ovarian clear cell carcinoma

Immunostaining intensity score	Number of cases	%
0	16	18
1+	53	60
2+	19	21
3+	1	1
4+	0	0
Total	89	100

Table 2

Correlation of Rsf-1 expression with clinical characteristics in ovarian clear cell carcinomas

Clinical characteristics	Rsf-1 (HBXAP) expression		
	Positive	Negative	*P*
Age (n=89)			
≥ 50	46 (79%)	12 (21%)	
< 50	27 (87%)	4 (13%)	0.36
Stage (n = 67)			
I, II	34 (72%)	13 (28%)	
III, IV	20 (100%)	0 (0%)	0.0088*
Peritoneal dissemination (n = 79)			
Negative	53 (80%)	13 (20%)	
Positive	12 (92%)	1 (8%)	0.30
Lymph node metastasis (n = 70)			
Negative	40 (73%)	15 (27%)	
Positive	15 (100%)	0 (0%)	0.023*
Survival status (n = 89)			
Alive	58 (81%)	14 (19%)	
Deceased	15 (88%)	2 (12%)	0.46

* statistically significant

Med Oncol
DOI 10.1007/s12032-011-9878-z

LETTER TO THE EDITOR

Second-line chemotherapy with docetaxel and carboplatin in paclitaxel and platinum-pretreated ovarian, fallopian tube, and peritoneal cancer

Takahide Arimoto · Shunsuke Nakagawa · Katsutoshi Oda · Kei Kawana · Toshiharu Yasugi · Yuji Taketani

Abstract We retrospectively evaluated the efficacy and toxicity of docetaxel and carboplatin in patients with platinum and paclitaxel-pretreated recurrent ovarian, fallopian tube, and peritoneal cancer. Forty-two women (38 with ovarian cancer, 1 with fallopian tube cancer, 3 with peritoneal cancer) whose cancer had progressed within 12 months of their last treatment with both a platinum agent and paclitaxel were treated with docetaxel (70 mg/m^2, day 1) and carboplatin (area under the curve of 4–6, day 1). Thirty-four patients had measurable disease. The objective response rate was 23% within 0–6 months of the progression-free interval, 50% within 6–12 months, and 32% (11 of 34 patients) for both groups. The median time to tumor progression was 28, 49, 34 weeks, and the median overall survival time was 94, 224, 111 weeks, respectively. The most common toxicity was grade 3/4 neutropenia (98% of patients), with 15 episodes (8.4% of courses) of neutropenic fever. The main nonhematologic toxicity was hypersensitivity; 7 patients (17%) required discontinuation of the therapy. The results of our study indicate that the combination of docetaxel and carboplatin is effective against recurrent ovarian, fallopian tube, and peritoneal cancer with progression-free interval of 6–12 months from previous treatment by paclitaxel and platinum. On the other hand, single-agent chemotherapy would be better than this regimen considering its low response rate and severe hematological toxicity for patients with progression-free interval less than 6 months.

T. Arimoto (✉) · S. Nakagawa · K. Oda · K. Kawana · T. Yasugi · Y. Taketani
Department of Obstetrics and Gynecology, Faculty of Medicine, The University of Tokyo, 7-3-1 Hongo, Bunkyo-ku, Tokyo 113-8655, Japan
e-mail: tarimoto-tky@umin.ac.jp

Published online: 06 March 2011

Keywords Docetaxel · Carboplatin · Chemotherapy · Early progression · Recurrent ovarian cancer

The standard regimen as second-line chemotherapy in recurrent ovarian cancer has not been established, especially in the patients with a short progression-free interval from the previous treatment. Docetaxel is an active drug as second-line chemotherapy for recurrent ovarian cancer as well as pegylated liposomal doxorubicin, irinotecan, topotecan, gemcitabine, and etoposide [1].

The purpose of this study was to evaluate activity and toxicity of the combination of docetaxel and carboplatin retrospectively in patients with paclitaxel and platinum resistant (progression-free interval less than 6 months) and partially resistant (progression-free interval of 6–12 months) ovarian, fallopian tube, and peritoneal cancers. Forty-two women (38 with ovarian cancer, 1 with fallopian tube cancer, 3 with peritoneal cancer) whose cancer had progressed within 12 months of their last treatment with both a platinum agent and paclitaxel were treated with docetaxel (70 mg/m^2, day 1) and carboplatin (area under the curve of 4–6, day 1). Thirty-four (81%) patients had measurable disease. Twenty-six (62%) patients had experienced progression of disease within less than 6 months of their last treatment, whereas 16 patients (38%) within 6–12 months. The median number of courses of treatment per patient was 4.5 (range: 1–8 courses). The median follow-up period was 107 weeks (range: 9–373 weeks). The objective response rate was 23% within 0–6 months of the progression-free interval, 50% within 6–12 months, and 32% (11 of 34 patients) for both groups. The median time to tumor progression was 28, 49, and 34 weeks, and the median overall survival time was 94, 224, and 111 weeks, respectively. The most common toxicity was grade 3/4 neutropenia (98% of patients), with 15 episodes

(8.4% of courses) of neutropenic fever. The main nonhematologic toxicity was hypersensitivity; 7 patients (17%) required discontinuation of the therapy. On the other hand, grade 2/3 neuropathy was observed only in two (4.8%) patients.

Several chemotherapeutic agents such as pegylated liposomal doxorubicin, topotecan, irinotecan, gemcitabine, and etoposide have been used in the treatment of platinum-resistant disease with response rates in the range 10–15% [2–5]. The results from our study about overall response rate are in line with other chemotherapeutic agents. Notably, our data about median time to tumor progression and overall survival are longer than the previously reported data of other regimens.

The results of our study indicate that the combination of docetaxel and carboplatin is effective against recurrent ovarian, fallopian tube, and peritoneal cancer with progression-free interval of 6–12 months from previous treatment by paclitaxel and platinum. On the other hand, single-agent chemotherapy would be better than this regimen considering its low response rate and severe hematological toxicity for patients with progression-free interval less than 6 months. However, chemotherapy with docetaxel and carboplatin may improve time to tumor progression and overall survival time in these cases; this regimen can be an alternative in patients whose hematological toxicity is relatively weak at their previous treatment.

Conflict of interest None.

References

1. Sugiyama T. Second-line chemotherapy for recurrent ovarian cancer. Gan To Kagaku Ryoho. 2005;32:28–32.
2. Swisher EM, Mutch DG, Rader JS, Elbendary A, Herzog TJ. Topotecan in platinum- and paclitaxel-resistant ovarian cancer. Gynecol Oncol. 1997;66:480–6.
3. Gordon AN, Tonda M, Sun S, Rackoff W. Long-term survival advantage for women treated with pegylated liposomal doxorubicin compared with topotecan in a phase 3 randomized study of recurrent and refractory epithelial ovarian cancer. Gynecol Oncol. 2004;95:1–8.
4. Mutch DG, et al. Randomized phase III trial of gemcitabine compared with pegylated liposomal doxorubicin in patients with platinum-resistant ovarian cancer. J Clin Oncol. 2007;25:2811–8.
5. Ferrandina G, et al. Phase III trial of gemcitabine compared with pegylated liposomal doxorubicin in progressive or recurrent ovarian cancer. J Clin Oncol. 2008;26:890–6.

Morita et al. Reproductive Biology and Endocrinology 2012, 10:14
http://www.rbej.com/content/10/1/14

REPRODUCTIVE BIOLOGY AND ENDOCRINOLOGY

RESEARCH Open Access

Resveratrol promotes expression of SIRT1 and StAR in rat ovarian granulosa cells: an implicative role of SIRT1 in the ovary

Yoshihiro Morita[1], Osamu Wada-Hiraike[1*], Tetsu Yano[1], Akira Shirane[1], Mana Hirano[1], Haruko Hiraike[1], Satoshi Koyama[1], Hajime Oishi[1], Osamu Yoshino[1], Yuichiro Miyamoto[1], Kenbun Sone[1], Katsutoshi Oda[1], Shunsuke Nakagawa[2], Kazuyoshi Tsutsui[3] and Yuji Taketani[1]

Abstract

Background: Resveratrol is a natural polyphenolic compound known for its beneficial effects on energy homeostasis, and it also has multiple properties, including anti-oxidant, anti-inflammatory, and anti-tumor activities. Recently, silent information regulator genes (Sirtuins) have been identified as targets of resveratrol. Sirtuin 1 (SIRT1), originally found as an NAD^+-dependent histone deacetylase, is a principal modulator of pathways downstream of calorie restriction, and the activation of SIRT1 ameliorates glucose homeostasis and insulin sensitivity. To date, the presence and physiological role of SIRT1 in the ovary are not known. Here we found that SIRT1 was localized in granulosa cells of the human ovary.

Methods: The physiological roles of resveratrol and SIRT1 in the ovary were analyzed. Immunohistochemistry was performed to localize the SIRT1 expression. SIRT1 protein expression of cultured cells and luteinized human granulosa cells was investigated by Western blot. Rat granulosa cells were obtained from diethylstilbestrol treated rats. The cells were treated with increasing doses of resveratrol, and subsequently harvested to determine mRNA levels and protein levels. Cell viability was tested by MTS assay. Cellular apoptosis was analyzed by caspase 3/7 activity test and Hoechst 33342 staining.

Results: SIRT1 protein was expressed in the human ovarian tissues and human luteinized granulosa cells. We demonstrated that resveratrol exhibited a potent concentration-dependent inhibition of rat granulosa cells viability. However, resveratrol-induced inhibition of rat granulosa cells viability is independent of apoptosis signal. Resveratrol increased mRNA levels of SIRT1, LH receptor, StAR, and P450 aromatase, while mRNA levels of FSH receptor remained unchanged. Western blot analysis was consistent with the results of quantitative real-time RT-PCR assay. In addition, progesterone secretion was induced by the treatment of resveratrol.

Conclusions: These results suggest a novel mechanism that resveratrol could enhance progesterone secretion and expression of luteinization-related genes in the ovary, and thus provide important implications to understand the mechanism of luteal phase deficiency.

Keywords: SIRT1, Resveratrol, Ovary, Granulosa cells, Luteinization

* Correspondence: osamu.hiraike@gmail.com
[1]Department of Obstetrics and Gynecology, Graduate School of Medicine, The University of Tokyo, 7-3-1, Hongo, Bunkyo-ku, Tokyo 113-8655, Japan
Full list of author information is available at the end of the article

Background

The study of natural compounds with pharmacological activity has become an emerging trend in nutritional and pharmacologic research. Polyphenols represent a vast group of compounds having aromatic ring, characterized by the presence of one or more hydroxyl groups with various structural complexities. Resveratrol (trans-3, 5, 40-trihydroxystilbene) is a natural polyphenol synthesized by plants as a phytoalexin that becomes activated under stress conditions such as ultraviolet radiation and fungal infection [1,2]. It can be found in berries, nuts and some medicinal plants, and mainly present in the skin of grapes and thus in red wine [3]. Previous studies have reported its anti-oxidant, anti-inflammatory, and growth-inhibitory activities using several cancer cell lines and animal models [2,4,5]. These properties of resveratrol have been linked to the inhibition of proliferation in association with cell cycle arrest and apoptotic cell death typically observed in vitro at concentrations in the range of 10-300 μM [5-7]. Thus, resveratrol has activity in regulating multiple cellular events associated with carcinogenesis, and the activation of SIRT1 is postulated to be a key event to elucidate the pathophysiology of resveratrol [8,9]. SIRT1, the mammalian homologue of yeast Sir2 (silent information regulator 2), functions as an NAD^+-dependent class III histone deacetylase. SIRT1 deacetylates multiple targets in mammalian cells, including p53, FOXO1, FOXO3, PGC-1α, liver X receptor, NBS1 and hypoxia-inducible factor 2α [10,11]. By regulating these molecules, SIRT1 functions as a master regulator of energy homeostasis, gene silencing, metabolism, genomic stability, and cell survival.

The ability of the ovary to produce growing follicles that ovulate is the basis of female fertilization. A critical feature of ovarian granulosa cell (GC) function is the differentiation of the ovulatory follicle into the corpus luteum which mainly produces progesterone (P4) that is important for the maintenance of pregnancy. Recently, it has been suggested that SIRT1 activator resveratrol plays a role in reproductive biology. Resveratrol was shown to modulate theca cell proliferation [12], and methylated resveratrol analogues possessed biological activities in swine GCs [13]. In the present study, to assess a role of SIRT1 in the regulation of reproductive axis in female, we investigated the expression of endogenous SIRT1 in human and rat GCs and the effect of resveratrol on cellular viability and steroidogenesis in rat GCs.

Methods

Chemicals

Diethylstilbestrol (DES) and resveratrol were purchased from Sigma-Aldrich (St. Louis, MO, USA). All other chemicals, unless otherwise mentioned, were obtained from Sigma-Aldrich.

Human cancer cell lines and primary human GCs

Human cervical cancer cell line HeLa was purchased from American Type Culture Collection (Manassas, VA, USA). Human ovarian granulosa-like tumor cell line KGN, which originated from a Stage III granulosa cell carcinoma in a 63-year-old Japanese women [14], was obtained from RIKEN Cell Bank of Japan (Tsukuba, Japan). Primary human GCs were obtained from patients undergoing transvaginal oocyte retrieval for in vitro fertilization at the University of Tokyo Hospital. The method to purify human GCs was described previously [15]. The study was approved by the Institutional Review Board of the University of Tokyo, and written informed consent for the research use of human GCs was obtained from each patient. These cells were maintained in Dulbecco's modified Eagle Medium (DMEM)/F12 medium (Invitrogen, Carlsbad, CA, USA) supplemented with 10% charcoal-stripped fetal bovine serum (FBS; Invitrogen), 100 U/ml penicillin, 100 μg/ml streptomycin and 0.25 μg/ml amphotericin B in a humidified atmosphere of 5% CO_2 and 95% air at 37°C.

Preparation and culture of rat GCs

Guidelines for the care and use of laboratory animals as adopted and promulgated by the University of Tokyo were followed. Twenty-three-day-old immature female Wistar rats were purchased from CLEA Japan, Inc. (Tokyo, Japan) and housed in a temperature-controlled room with a 12 h light/12 h dark schedule. Pelleted food and water were provided ad libitum. Rats were implanted with SILASTIC capsules (Dow Corning, Corp., Midland, MI, USA) containing 10 mg DES to increase GC number [16], and killed 4 days later by cervical dislocation. Removed ovaries were immediately cleaned of surrounding connective tissues and placed into DMEM/F12 medium supplemented with 10% charcoal-stripped FBS, 100 U/ml penicillin, 100 μg/ml streptomycin and 0.25 μg/ml amphotericin B. GCs were harvested by needle puncture of ovarian follicles, suspended in the medium, and purified by filtration with a 100-μm cell strainer and then a 40-μm cell strainer (BD Biosciences, Bedford, MA, USA). Isolated GCs were washed twice by centrifugation at 200 × g for 5 min and cultured in the medium in a humidified atmosphere of 5% CO_2 and 95% air at 37°C [17].

Tissue samples and immunohistochemistry

The ovarian tissues used in this study were obtained from 5 female patients with regular menstrual cycles who were taking no hormonal drugs and underwent

radical or extended hysterectomy for carcinoma of the uterine cervix and endometrium. The female patients were 32-44 years old at the time of operation and the operations were performed in proliferative phase of the menstrual cycle. The study was approved by the Institutional Review Board of the University of Tokyo, and written informed consent was obtained in each instance. Immunohistochemistry was performed as described previously [18]. Paraffin sections (4 μm) were dewaxed in xylene and rehydrated through graded ethanol to water. Antigens were retrieved by boiling in 10 mM citrate buffer (pH 6.0) for 30 min. The cooled sections were incubated in DAKO REAL Peroxidase-Blocking solution (DAKO, Carpinteria, CA, USA) for 30 min to quench endogenous peroxidase. To block the nonspecific binding, sections were incubated in PBS containing 3% BSA and 0.5% Nonidet P-40 for 10 min at room temperature. Sections were then incubated with the rabbit polyclonal antibody to SIRT1 (sc-15404, Santa Cruz Biotechnology, Inc., Santa Cruz, CA, USA) in DAKO REAL Antibody Diluent (DAKO) overnight at 4°C. Negative controls were incubated with preimmune serum IgG fraction. ChemMate EnVision Detection system (DAKO) was used to visualize the signal. The sections were developed with 3,3'-diaminobenzidine tetrahydrochloride substrate (DAKO), lightly counterstained with ae's hematoxylin (Wako Chemical, Tokyo, Japan), dehydrated through ethanol series and xylene, and mounted.

Western blotting

HeLa cells, KGN cells, and human GCs were seeded into 6-cm culture dishes (BD Biosciences) at a density of 1×10^6 cells/dish in 3 ml of the culture medium. After 48 h, the cells were harvested with trypsin (0.05%)/EDTA (0.02%) and scraped into the lysis buffer containing 50 mM Tris-HCl (pH 8.0), 150 mM NaCl, 0.02% sodium azide, 0.1% sodium dodecyl sulfate, 1% Nonidet P-40, and 0.5% sodium deoxycholate for 30 min on ice. Rat GCs were seeded into 10-cm culture dishes (BD Biosciences) at a density of $2\text{-}3 \times 10^6$ cells/dish in 10 ml of the culture medium. After 48 h, the medium was replaced with fresh medium containing 1% charcoal-stripped FBS and 100 μM of resveratrol, and cell culture was continued. Thereafter GCs were harvested, and lysed. Insoluble material was removed by centrifugation at 12,000 × g, for 20 min at 4°C. The supernatants were recovered, and the protein concentrations were measured using Bio-Rad protein assay reagent (Bio-Rad Lab., Hercules, CA, USA). Equivalent amounts of lysate protein (30 μg were subjected to 10% SDS-PAGE and electrophoretically transferred onto polyvinylidene difluoride membranes (Millipore Corp., Billerica, MA, USA). After blocking nonspecific binding sites by incubation for 1 h with Tris-buffered saline (25 mM Tris and 150 mM NaCl, pH 7.6) containing 5% nonfat milk and 0.2% Tween 20, the membranes were blotted with the primary antibodies overnight at 4°C. The primary antibodies used were anti-DBC1 [19] and anti-P450 aromatase (P450arom; MCA2077S, AbD serotec, Oxford, UK). Anti-SIRT1 (sc-15404), anti-StAR (sc-25806), and anti-LH receptor (LH-R; sc-25828) were purchased from Santa Cruz Biotechnology Inc. (Santa Cruz). Reactive proteins were detected with horseradish peroxidase-conjugated secondary antibodies (Cell Signaling Technology, Inc., Beverly, MA, USA) for 60 min at room temperature and developed with ECL Plus western blotting detection reagents (GE Healthcare, Little Chalfont, UK). The membranes were stripped with the buffer containing 100 mM 2-mercaptoethanol, 2% SDS and 62.5 mM Tris- HCl (pH 6.7), then reprobed with mouse monoclonal antibody to β-Actin (sc-47778, Santa Cruz Biotechnology, Inc.) to confirm equivalent protein loading. The images were scanned by the luminescent image analyzer Image Quant LAS 4000 mini (GE Healthcare).

Granulosa cell progesterone production

Culture media for the Western blot were collected, frozen, and stored at -20°C until P4 determination by Progesterone EIA kit (Cayman Chemical Co., Ann Arbor, MI, USA). P4 assay was performed according to the manufacture's instruction. The data are expressed as the amount of steroids (pg/ml) secreted. The results are representative of three to four independent cultures with each condition in quadruplet.

Cell viability assay

Viability of rat GCs was examined by using the 3-(4,5-dimethylthiazol-2-yl)-5- (3-carboxymethoxyphenyl)-2-(4-sulfophenyl)-2H-tetrazolium, inner salt (MTS) assay kit (CellTiter 96 Aqueous One Solution Cell Proliferation Assay; Promega, Madison, WI, USA) according to the manufacturer's instructions. Briefly, cells were seeded into 96-well plates (BD Biosciences) at a density of 1×10^4 cells/well in 100 μL of the culture medium. After 48 h, the medium was replaced with fresh medium containing 1% charcoal-stripped FBS and various concentrations of resveratrol, and cell culture was continued for a further 72 h. Resveratrol was dissolved in dimethyl sulfoxide and diluted with the medium to yield desired concentrations. The final concentration of dimethyl sulfoxide never exceeded 0.05%. The effects of resveratrol were investigated at concentrations between 10 and 100 μM in consideration of those used in the other studies where resveratrol inhibited the proliferation of various cell types at concentrations in the range of 10-300 μM [5-7]. Finally, the medium was replaced with 100 μL of fresh medium containing 20 μL of MTS solution and incubated for an additional 4 h. Mitochondrial

dehydrogenase enzymes of viable cells converted MTS tetrazolium into a colored formazan product. The optical density of samples was read at 490 nm in the spectrophotometric microplate reader (BioTek, Winooski, VT, USA).

Reverse transcription and quantitative real-time PCR

Rat GCs were seeded into 6-cm culture dishes (BD Biosciences) at a density of 1×10^6 cells/dish in 3 ml of the culture medium. After 48 h, the medium was replaced with fresh medium containing 1% charcoal-stripped FBS and various concentrations of resveratrol (10-100 μM, and cell culture was continued for a further 24 h. Total cellular RNA was extracted using RNeasy Mini Kit (Qiagen, Hilden, Germany) and quantified by measuring absorbance at 260 nm and stored at -80° until assay. The mRNA levels of relevant molecules were measured by quantitative real-time RT-PCR using One Step SYBR PrimeScript RT-PCR Kit (TaKaRa Bio. Inc., Tokyo, Japan) in the Light Cycler (Roche Applied Science, Mannheim, Germany). Accumulated levels of fluorescence were analyzed by the second-derivative method after the melting-curve analysis, and then the expression levels of target genes were normalized to the expression level of β-Actin in each sample. Primer pairs of analyzed mRNA are described in Table 1.

Table 1 Primer sequences used for quantitative real-time PCR

Gene	Primers	Primer Sequence	Expected size in base pair
β-actin	Sense	CGAGTACAACCTTCTTGCAG	207
	Antisense	TTCTGACCCATACCCACCAT	
Bax	Sense	GAATTGGCGATGAACTGGAC	157
	Antisense	GCAAAGTAGAAAAGGGCAACC	
Bcl2	Sense	AACATCGCTCTGTGGATGAC	150
	Antisense	GAGCAGCGTCTTCAGAGACA	
DBC1	Sense	TCTCCAAGTCTCGCCTGTG	158
	Antisense	CTCTGTTGCCTCCAACCAGT	
FSH-R	Sense	ATGGCCCCCATTTCATTCTT	82
	Antisense	ACTAGGAGAATCTTGGCCTTGGA	
LH-R	Sense	ATTGACACTCTGCTTAACTTTCCATCT	82
	Antisense	TGGCCATGAGGTACTCATGATCT	
p450arom	Sense	TCCTCAGCAGAGAAACTGGAAGA	151
	Antisense	CGTACAGAGTGACGGACATGGT	
SIRT1	Sense	TGTTTCCTGTGGGATACCTGA	137
	Antisense	TGAAGAATGGTCTTGGGTCTTT	
StAR	Sense	AGGAAAACAGAACTGAGGCTTAGAATA	93
	Antisense	AAGGTTTCATAGATACCTGTCCCTTAAC	

Caspase-3/7 activity assay

Apoptosis executioner caspase-3/7 activity in rat GCs was measured using the Apo-ONE Homogeneous Caspase-3/7 Assay kit (Promega) according to the manufacturer's instructions. Briefly, cells were seeded into 96-well plates (BD Biosciences) at a density of 1×10^4 cells/well in 100 μL of the culture medium. After 48 h, the medium was replaced with fresh medium containing 1% charcoal-stripped FBS and various concentrations of resveratrol (10- 100 μM), and cell culture was continued for 6, 12 and 24 h. Caspase-3/7 activity was measured at excitation wavelength 485 nm and emission wavelength 528 nm in the spectrophotometric microplate reader (BioTek).

Hoechst 33342 nuclear staining

Hoechst staining was performed to confirm the apoptotic profile as a result of morphological change in the nucleus in which Hoechst 33342 binds specifically to A-T base region in DNA and emits fluorescence. Rat GCs were seeded into 8-well chamber slides (Nalge Nunc International, Naperville, IL, USA) at a density of 1×10^5 cells/well in 400 μl of the culture medium. After 48 h, the medium was replaced with fresh medium containing 1% charcoal-stripped FBS and resveratrol (50 and 100 μM), and cell culture was continued for 6, 12, 24 and 48 h. Finally, cells were rinsed in PBS and fixed with 4% paraformaldehyde in PBS (pH 7.4) at room temperature for 30 min. Then cells were rinsed in PBS twice and stained with Hoechst 33342 (10 μg/ml in PBS) for 3 min. The specimens were mounted with Vectashield medium (Vector Labs. Inc., Burlingame, CA, USA) and photographs were taken at X200 magnification under a fluorescent confocal microscope (Carl-Zeiss MicroImaging Inc., Oberkochen, Germany).

Statistical analysis

Data represent the mean ± SEM from at least three independent experiments. Statistical analyses were carried out by one-way ANOVA with *post-hoc* test for multiple comparisons by using StatView software (SAS Institute Inc., Cary, NC, USA). $P < 0.05$ was considered statistically significant.

Results

Expression of SIRT1 protein in human GCs

We investigated the localization of SIRT1 protein in the human ovary using immunohistochemistry. Expression of SIRT1 was observed in nuclei of GCs at various stages of follicular development (Figure 1A-C). Part of the theca interstitial cells and the oocyte were also found to have positive signals. To confirm the expression of SIRT1, luteinized human granulosa cells were obtained from women undergoing in vitro fertilization

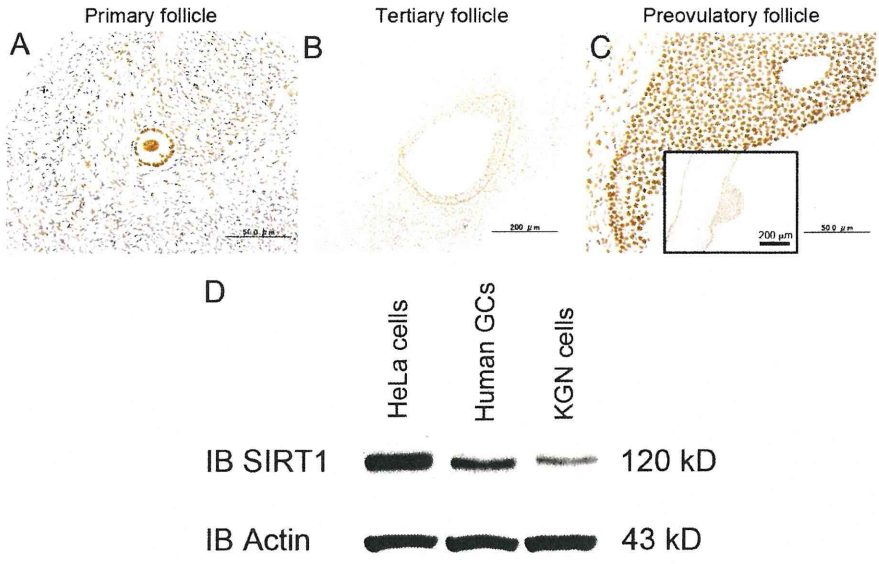

Figure 1 Expression of SIRT1 protein in human GCs. Immunohistochemical detection of SIRT1 in the human ovary (A, primary follicle; B, tertiary follicle; C, preovulatory follicle). Representative data from five specimens were shown. Nuclei of GCs were positively stained with anti-SIRT1 antibody at various stages of follicular development. Bars indicate (A) 50 μm, (B) 200 μm, and (C) 50 μm in high-power field and 200 μm in low-power field. SIRT1 was detected in primary (A), tertiary (B), and preovulatory (C) follicles of granulosa cells. Note that a part of the theca cells and oocyte nucleus are stained. Negative controls included a section incubated with preimmune rabbit IgG. (D) Western blotting revealed the presence of SIRT1 in KGN cells, human GCs, and HeLa cells (positive control).

program, and Western blot analysis revealed the expression of SIRT1 protein in KGN cells and human GCs (Figure 1D). HeLa cells were used as a positive control for Western blot because we [19] and other investigators [20] have detected the expression of SIRT1 protein.

Effect of resveratrol on cell viability and expression of SIRT1 and DBC1 in cultured rat GCs

To determine whether activation of SIRT1 by resveratrol affects rat GC viability, the extent of cell viability was measured by MTS assay. Resveratrol, at concentrations between 50 and 100 μM, produced a dose-dependent inhibition of cell viability after 72 h of treatment, with the maximal effect (reduction to 22.8 ± 4.4% of the control) being observed at 100 μM (Figure 2A). Recent studies have shown that DBC1 promotes p53-mediated apoptosis through specific inhibition of deacetylase activity of SIRT1 [21,22]. To determine whether the inhibitory effect on cell viability by resveratrol is related to the change in SIRT1 activation, the effect of resveratrol on mRNA levels of SIRT1 and DBC1, a negative regulator of SIRT1, was investigated by quantitative real-time RT-PCR in cultured rat GCs. After 24 h culture of rat GCs, mRNA levels of SIRT1 significantly increased at 100 μM (Figure 2B), while those of DBC1 remained unchanged (Figure 2C). Western blot analysis was also performed to confirm the result of quantitative real time RT-PCR and resveratrol-dependent induction of SIRT1 protein was observed (Figure 2D)

Effect of resveratrol on cell-death machinery in cultured rat GCs

Resveratrol has been shown to induce cell-cycle arrest and apoptosis in various cell lines [5,12]. To determine whether the reduction of the viability of rat GCs by resveratrol is due to the induction of apoptosis, the effect of resveratrol on mRNA levels of the representative apoptosis promoter Bax and inhibitor Bcl-2 was analyzed by quantitative real-time RT-PCR in cultured rat GCs at concentrations of resveratrol between 10 and 100 μM. The significant change in mRNA levels of Bax and Bcl-2 was not found at 24 h (Figure 3A, B). Apoptosis executioner caspase-3/7 activity was measured in cultured rat GCs at concentrations of resveratrol ranging from 10 to 100 μM and at various time points (6, 12, and 24 h). Resveratrol significantly inhibited caspase-3/7 activity at 75 and 100 μM after 24 h of treatment (Figure 3C). Furthermore, the effect of resveratrol on the incidence of apoptotic cells was investigated by Hoechst 33342 nuclear staining. Resveratrol (50 and 100 μM) showed no typical apoptotic changes including nuclear shrinkage, chromatin condensation, and nuclear fragmentation in cultured rat GCs at 6, 12, 24, and 48 h (Figure 3D).

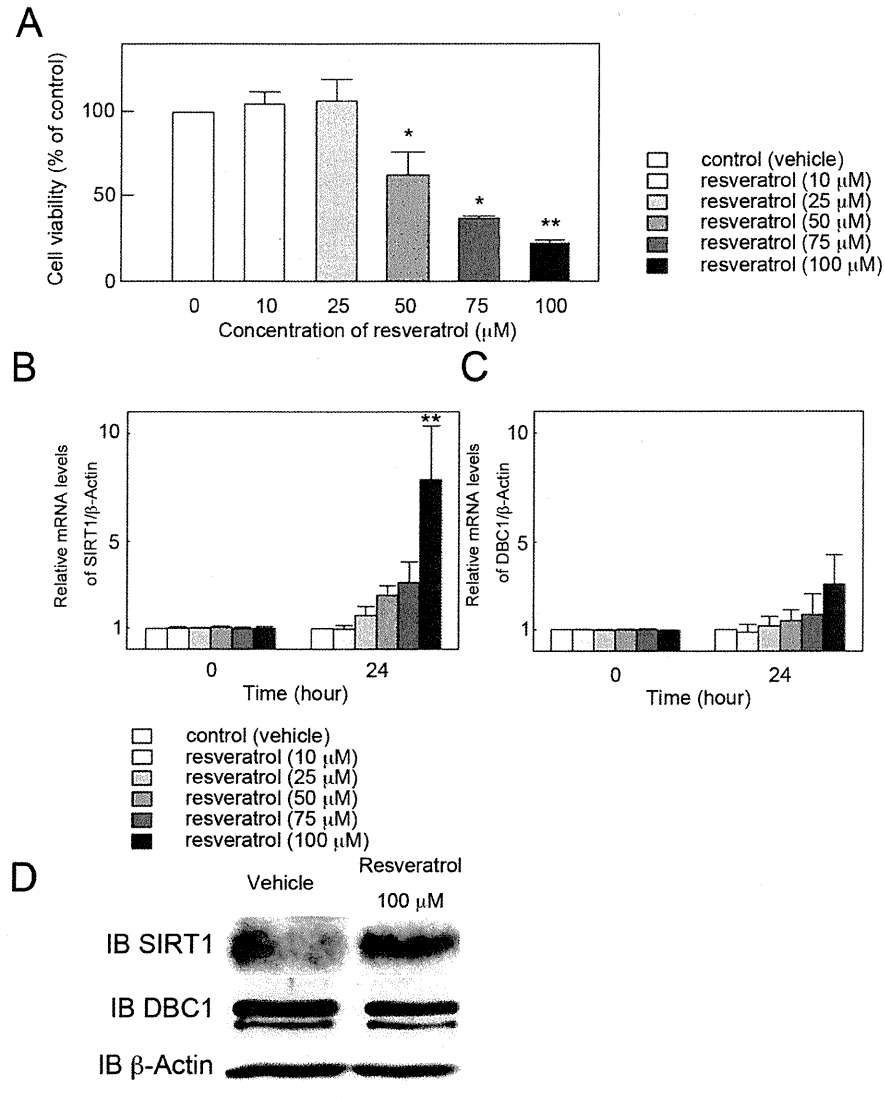

Figure 2 Effect of resveratrol on cell viability and expression of SIRT1 and DBC1 in cultured rat GCs. (A) Effect of resveratrol on cell viability at 72 h was estimated by MTS assay. Results are shown as the mean percentage of the untreated control ± SEM (bars) of eight wells of three independent experiments * $p < 0.05$ *vs.* control. ** $p < 0.01$ *vs.* control. (B and C) Effect of resveratrol on mRNA levels of (B) SIRT1 and (C) DBC1 was investigated by quantitative real-time RT-PCR. The mRNA level of the untreated control was arbitrarily set at 1.0, and that of the treatment group was estimated relative to the control value. Results are shown as the mean ± SEM (bars) of three independent experiments. ** $p < 0.01$ *vs.* control. (D) Effect of resveratrol on protein levels of SIRT1 was investigated by Western blot. Resveratrol treatment resulted in an increased expression of SIRT1 protein, and the results were consistent with that of quantitative real time RT-PCR. Three independent experiments were performed and a representative result is shown.

Effect of resveratrol on folliculogenesis-related molecules in cultured rat GCs

The Effect of resveratrol on mRNA levels of folliculogenesis-related molecules was investigated by quantitative real-time RT-PCR in cultured rat GCs at concentrations of resveratrol between 10 and 100 μM. After 24 h culture, resveratrol significantly increased mRNA levels of LH-R, steroidogenic acute regulatory protein (StAR), and P450arom at 100 μM (Figure 4B-D), while FSH receptor (FSH-R) mRNA levels remained unchanged (Figure 4A). Western blot analysis was also performed to confirm the result of quantitative real time RT-PCR and resveratrol-dependent stimulation of StAR, LH-R, and P450arom protein was confirmed (Figure 4E). To investigate the possibility that resveratrol promote steroidgenesis, serum concentration of P4 was evaluated and it has been revealed that resveratrol exhibited 3-fold enhancement of hormonal secretion at 48 h of culture (Figure 4F).

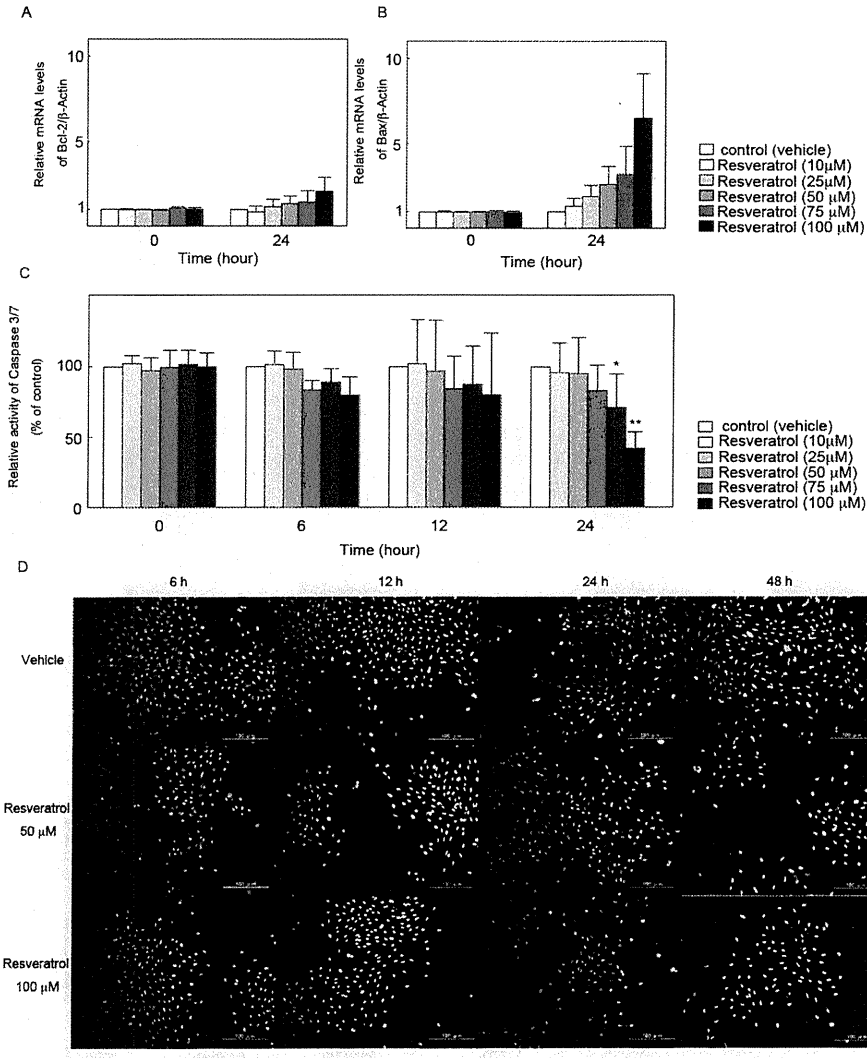

Figure 3 Effect of resveratrol on cell-death machinery in cultured rat GCs. Effect of resveratrol on mRNA levels of (A) Bcl-2 and (B) Bax was investigated by quantitative real-time RT-PCR. The mRNA level of the untreated control was arbitrarily set at 1.0, and that of the treatment group was estimated relative to the control value. Results are shown as the mean ± SEM (bars) of three independent experiments. (C) Caspase-3/7 activity was measured by the Apo-ONE Homogeneous Caspase-3/7 Assay kit at 6, 12 and 24 h. Results are shown as the mean percentage of the untreated control ± SEM (bars) of eight wells of three independent experiments. (D) Hoechst 33342 staining of resveratrol-treated rat GCs at 6, 12, 24, and 48 h. * $p < 0.05$ *vs.* control. ** $p < 0.01$ *vs.* control.

Discussion

Recently, resveratrol has been the focus of many *in vitro* and *in vivo* studies because of its pleiotropic biological activities [1-9]. However, the studies of resveratrol in ovarian physiology are limited. Resveratrol has been reported to exert estrogenic effects, increasing uterine and ovarian wet weight [23]. It is a phytoestrogen known to bind equally to estrogen receptors α and β [24], and structurally similar to synthetic estrogens, such as DES and 17β-estradiol benzoate [25]. In contrast to its hyperproliferative effects, resveratrol promoted apoptosis in rat ovarian theca-interstitial cells [12], and its analogues inhibited swine GC growth [13]. It was also reported that resveratrol inhibited the proliferation of a wide variety of human cancer cell lines through the induction of S-phase cell cycle arrest and apoptosis [5]. In the present study, we demonstrated that resveratrol exerted a dose-dependent inhibition of cell viability on rat GCs. This effect appeared not to be due to the induction of apoptosis, which was different from the previous findings in rat ovarian theca-interstitial cells [12]. Then we studied whether this resveratrol-induced decrease of cellular viability may lead to the differentiation of GCs.

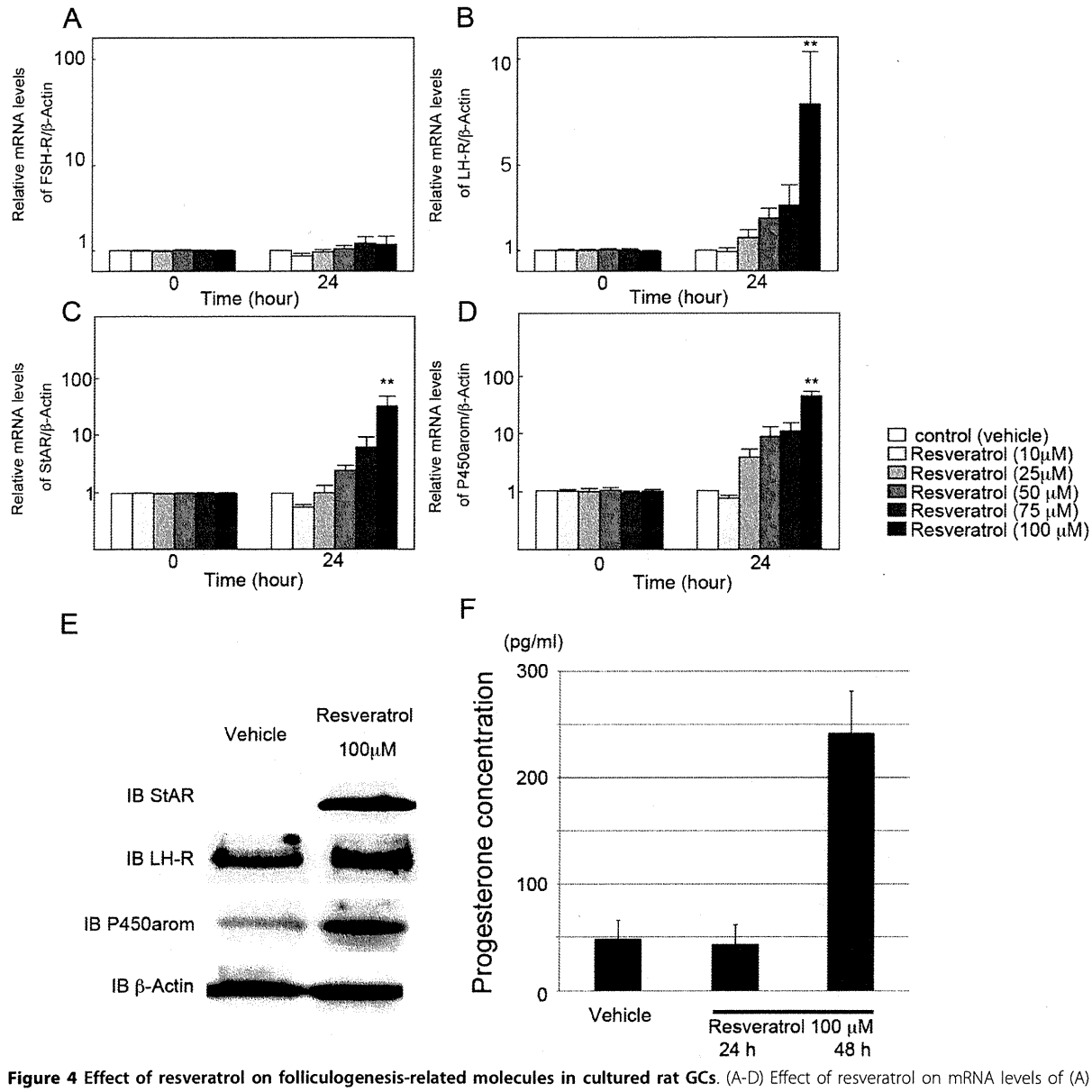

Figure 4 Effect of resveratrol on folliculogenesis-related molecules in cultured rat GCs. (A-D) Effect of resveratrol on mRNA levels of (A) FSH-R, (B) LH-R, (C) StAR and (D) P450arom was investigated by quantitative real-time RT-PCR. The mRNA level of the untreated control was arbitrarily set at 1.0, and that of the treatment group was estimated relative to the control value. Results are shown as the mean ± SEM (bars) of three independent experiments. ** $p < 0.01$ *vs.* control. (E) Effect of resveratrol on protein levels of StAR and P450arom was investigated by Western blot. Resveratrol treatment resulted in an increased expression of StAR, LH-R, and P450arom, and the results were consistent with those of quantitative real time RT-PCR. Three independent experiments were performed and a representative result is shown. (F) Effect of resveratrol on P4 secretion by rat granulosa cells. P4 secretion was measured by EIA protocol in culture medium of granulosa cells after 24 to 48 h of culture in DMEM/F-11 medium in the presence of resveratrol (100 μM). The data are expressed as the amount of steroids (pg/ml) secreted. The results, expressed as means ± SEM, are representative of three to four independent cultures with each condition in quadruplet.

Sirtuins are a conserved family of NAD^+-dependent class III histone deacetylases involved in a number of cellular processes including gene silencing at telomere and mating loci, DNA repair, recombination, and aging [8,10,11]. Recent studies have established that SIRT1 plays an important role in the regulation of cell fate and stress response in mammalian cells, and promotes cell survival by inhibiting apoptosis or cellular senescence induced by stresses including DNA damage [11]. Indeed, resveratrol administration and accompanying activation